COBEM 2023 27TH INTERNATIONAL CONGRESS OF MECHANICAL ENGENEERING

ABCM Brazilian Society of Mechanical Sciences and Engineering
27th ABCM International Congress of Mechanical Engineering
December 04-08, 2023, Florianópolis-SC, Brazil

COB-2023-1714
Characterization of two-dimensional reservoir based on transient pressure and temperature data using ensemble-based method

Jose Adriano Cardoso
Vinicius Mattoso Reis Da Silva
Danmer Maza
Márcio Carvalho
Laboratory of Microhydrodynamics and Flow in Porous Media, PUC-Rio, Rio De Janeiro, Brazil
jcardoso@lmmp.mec.puc-rio.br, vmatoso@lmmp.mec.puc-rio.br, danmer@lmmp.mec.puc-rio.br, msc@lmmp.mec.puc-rio.br

Abstract. *Important strategies for the production and management of an oil field are defined based on accurate characterization of the fluids and reservoir properties. Traditionally, pressure data from well tests and production have been made used to estimate reservoir permeability and porosity. However, in high transmissibility reservoirs, using only pressure data can lead to misinterpretations due to thermal effects and, therefore, errors in the reservoir characterization. Recent works on reservoir characterization have shown that the use of temperature transient data combined with pressure data produces better results. Reservoir parameters can be estimated by solving an inverse problem using the Ensemble Smoother with Multiple Data Assimilation (ES-MDA) method. Recent work using this methodology in a system consisting of a well coupled with a 1-D radial reservoir has shown the potential of this technique on reservoir parameter estimation workflow. This work extends previous analyses considering a producing well coupled with a 2-D non-homogeneous reservoir. The implemented method was able to accurately estimate the permeability and porosity of different regions within the reservoir.*

Keywords: *Reservoir Characterization, Inverse problem, ES-MDA*

1. INTRODUCTION

Well tests are usually performed to determine the rock properties of a reservoir and are commonly described by radial models, which have been successfully used despite the limitation of evaluating only radial property changes. In order to overcome this limitation, this work presents a numerical transient-thermal model for a coupled wellbore/2D Cartesian reservoir that takes into account the effects of Joule-Thompson heating/cooling, adiabatic fluid expansion/compression, conduction, and convection effects for both wellbore and reservoir for a single-phase fluid flow.

Commonly, the well test assumes an isothermal fluid flow into the reservoir; i.e., the temperature change is neglected, as presented by Park and Horne (1989). However, this assumption can lead to misinterpretation of pressure signal and as a consequence errors in the reservoir characterization especially in reservoirs at high transmissibility, as discussed by Galvao *et al.* (2020). Temperature measurement technology have advanced over the past few decades, offering measurements with excellent precision and resolution. As a result, a number of recent studies, including Sui *et al.* (2008), Onur and Cinar (2017) and Mattoso R. da Silva (2022), have suggested combined analyses of transient pressure and temperature data to enhance the information obtained from downhole gauges and more accurately characterize near-wellbore and far-field reservoir parameters.

The Ensemble Smoother with Multiple Data Assimilation (ES-MDA) method have been successfully applied in reservoir problems into the world of inverse problem because they are able to achieve acceptable data matches. This method creates multiple models to produce a confidence interval for the parameters. The results show that the ES-MDA method, when applied with the coupled pressure and temperature transient data, provides better reservoir characterization and uncertainty quantification, even in the presence of periodic disturbances introduced in pressure and temperature data.

2. MATHEMATICAL AND NUMERICAL FORMULATION

The mathematical formulation comprises a coupled wellbore/reservoir model, which consists of a fully coupled reservoir/casing/tubing system. In the reservoir, the mass and energy transient conservation equations in two dimensions are solved, denoted as Eq. (3) and Eq. (5) respectively. The wellbore model consists of mass, momentum, and energy transient conservation equations, represented by Eq. (7), Eq. (8), and Eq. (10). To solve the coupled wellbore/2D reservoir system, an accurate finite difference method was developed considering appropriate boundary conditions.

2.1 Coupled Wellbore-Reservoir system

2.1.1 Cartesian Reservoir

The reservoir model used in this work is based on the model presented by Onur and Cinar (2017), but here it is solved in Cartesian coordinates. The reservoir is considered heterogeneous, i.e. the permeability and porosity values may vary as a function of the "x" and "y" coordinates, as illustrated in Fig. 1.

The following hypotheses are considered:

- Flow in a Cartesian coordinate system;
- Single-phase oil with immobile connate water saturation;
- Reservoir may be heterogeneous and isotropic;
- Fluid flow is governed by Darcy's Law, in both directions;
- Reservoir parameters and fluid properties do not vary with temperature and pressure (except density and porosity);
- Wellbore is vertical and fully penetrates the reservoir;
- Solid matrix is in local thermal equilibrium with surrounding fluids (oil and water);
- The reservoir is thermally isolated;
- There is no fluid flow from boundaries;
- Gravity effects neglected.

Figure 1 shows a schematic drawing of the coupled wellbore/2D-reservoir system. Which consists of a vertical wellbore coupled in a Cartesian reservoir by the lower bottom corner. The reservoir exhibits three distinct permeability zones identified as $K1,\ K2,\ and\ K3$.

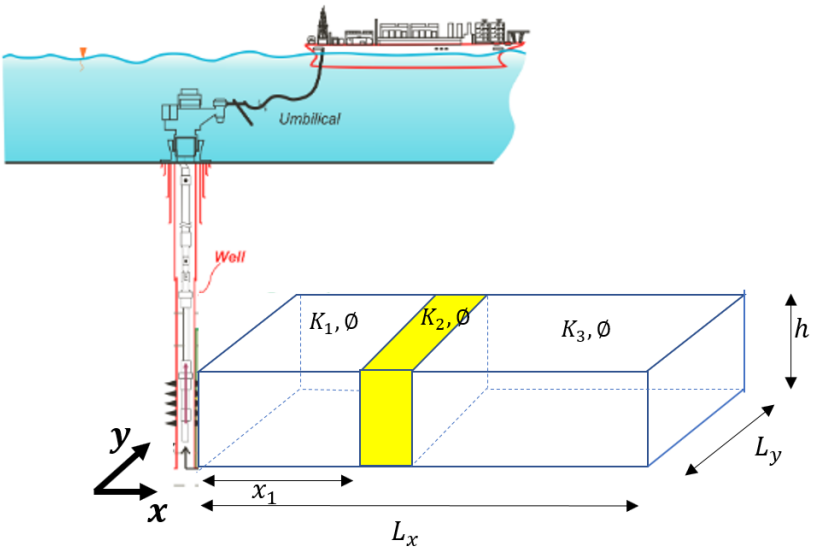

Figure 1: A schematic of the model description.

In the following sections of this paper, the mathematical formulation of the mass and energy equations of the reservoir will be presented. Starting with the mass conservation equation.

Mass Conservation equation

The mass balance of each phase (oil and water) is written as:

$$\frac{\partial}{\partial t}\left(\phi s_m \rho_m\right) + \nabla \cdot \left(\rho_m \mathbf{v}_m\right) = 0, \tag{1}$$

where $m = w, o$ and s_m is the saturation . Using the isothermal compressibility and isobaric thermal expansion coefficients for oil and water phases C_m & β_m, and also the effective isothermal compressibility, and isobaric thermal expansion coefficients for the rock, C_r & β_r,

$$C_m = \frac{1}{\rho_m}\frac{\partial \rho_m}{\partial p}\bigg|_T, \quad \beta_m = -\frac{1}{\rho_m}\frac{\partial \rho_m}{\partial T}\bigg|_p, \quad C_r = \frac{1}{\phi}\frac{\partial \phi}{\partial p}\bigg|_T, \quad \beta_r = -\frac{1}{\phi}\frac{\partial \phi}{\partial T}\bigg|_p. \tag{2}$$

Making the substitutions and combining the equations, we have the mass balance applied to the Cartesian flow in the porous media expressed as a function of pressure p and temperature T, as:

$$\frac{\partial p}{\partial t} - \frac{\beta_{tot}}{C_{tot}}\frac{\partial T}{\partial t} + \frac{1}{C_{tot}\phi}\frac{\partial v_x}{\partial x} + \frac{1}{C_{tot}\phi}\frac{\partial v_y}{\partial y} + \frac{C_o}{C_{tot}\phi}v_x\frac{\partial p}{\partial x} + \frac{C_o}{C_{tot}\phi}v_y\frac{\partial p}{\partial y} - \frac{\beta_o}{C_{tot}\phi}v_x\frac{\partial T}{\partial x} - \frac{\beta_o}{C_{tot}\phi}v_y\frac{\partial T}{\partial y} = 0 \tag{3}$$

In Equation (3), v_x and v_y represent Darcy's Law for each direction. C_{tot} and C_o are the total and oil phase compressibility, respectively. β_{tot} and β_o are the total and oil phase thermal expansion coefficient.

$$C_{tot} = C_r + s_w C_w + s_o C_o, \quad \beta_{tot} = \beta_r + s_w\beta_w + s_o\beta_o, \quad \mathbf{v}_m = \frac{-K_m}{\mu}\nabla(p). \tag{4}$$

Energy Conservation Equation

Assuming local thermal equilibrium between the solid matrix and fluid phase and including the Joule-Thomson coefficient (ϵ_{jTo}), the energy conservation proposed by (Onur *et al.*, 2017), and adapted to Cartesian coordinate in this work, can be expressed as:

$$\begin{aligned}\frac{\partial T}{\partial t} - \varphi_t^*\frac{\partial p}{\partial t} + C_{pRo}v_x\frac{\partial T}{\partial x} + C_{pRo}v_y\frac{\partial T}{\partial y} - C_{pRo}\epsilon_{jTo}v_x\frac{\partial p}{\partial x} - C_{pRo}\epsilon_{jTo}v_y\frac{\partial p}{\partial y} \\ - \frac{\partial}{\partial x}\left(\alpha_t\frac{\partial T}{\partial x}\right) - \frac{\partial}{\partial y}\left(\alpha_t\frac{\partial T}{\partial y}\right) = 0\end{aligned} \tag{5}$$

where φ_t^* represent the effective adiabatic expansion coefficient of the saturated-porous medium, C_{pRo} ratio of the volumetric heat capacity of the oil to the volumetric heat capacity of the fluid saturated rock, ϵ_{jTo} is the Joule-Thomson coefficient, and α_t is the thermal diffusivity of the fluid-saturated rock.

$$C_{pRo} = \frac{\rho_o c_{po}}{(\rho c_p)_t + \phi p\beta_r}, \quad \alpha_t = \frac{\lambda_t}{(\rho c_p)_t + \phi p\beta_r}, \quad \varphi^* = \frac{(\rho c_p\varphi)_t + \phi p C_r}{(\rho c_p)_t + \phi p\beta_r}. \tag{6}$$

In the following section, the wellbore model's underlying hypothesis will be listed, along with a brief explanation of the mass, momentum, and energy equations.

2.1.2 Wellbore Model

In the wellbore system, the conservative equations are based on models presented by Sui *et al.* (2008) and Onur and Cinar (2017). It considers the following assumptions:

- Axial flow of slightly compressible single-phase fluid;
- Wellbore storage is considered;
- Heat transfer to the surroundings occurs due to radial diffusion. There is no axial heat diffusion;
- Density is a function of temperature and pressure. Other fluid properties are constant;
- Wellbore materials have constant thermal conductivity.

Mass conservation equation

Introducing the volumetric flow rate, q, and considering positive the upward flow direction, the mass conservation equation proposed by Onur *et al.* (2017), can be expressed as:

$$\frac{\partial p}{\partial t} + \frac{q}{AC_o}\frac{\partial p}{\partial z} - \frac{\beta_o}{C_o}\frac{\partial T}{\partial t} - \frac{q\beta_o}{AC_o}\frac{\partial T}{\partial z} + \frac{1}{AC_o}\frac{\partial q}{\partial z} = 0 \tag{7}$$

In the wellbore, the pipe is considered rigid with a cross-sectional area A shown in Equation (7).

Momentum conservation equation

In this work, the conservation equations presented by Chaudhry (1979) and Mansoori et al. (2015), cited by Onur *et al.* (2017), are used. Assuming the well vertical (z) flow hypothesis, the radial direction (r) has the momentum neglected, and the momentum equation of the wellbore can be expressed by:

$$\frac{1}{A}\frac{\partial q}{\partial t} + \frac{q}{A^2}\frac{\partial q}{\partial z} + \frac{1}{\rho_o}\frac{\partial p}{\partial z} + \frac{fq|q|}{2A^2D} + gsin(\alpha) = 0 \tag{8}$$

In Equation (8), the angle (α) refers to the angle that the wellbore makes with the horizontal. Since we are considering a vertical well, $\alpha = 90°$. The variables D and f in Eq. (8) represent the inside diameter of the pipe and the Darcy-Weisbach friction factor, respectively.

$$\frac{1}{\sqrt{f}} = -2.0log\left(\frac{\delta/D}{3.7} + \frac{2.51}{R_e\sqrt{f}}\right), \quad R_e = \frac{\rho v_z D}{\mu} = \frac{v_z D}{\nu} = \frac{qD}{A\nu}, \tag{9}$$

Energy conservation equation

The heat exchange between the fluid inside the wellbore and the formation is similar to the one presented by Hasan and Kabir (2005). modeled by the following equation:

$$\rho_o A C_{po}(1 + C_T)\frac{\partial T}{\partial t} = \rho_o q C_{po} L_R\Big[T_{ext}(z) - T(z,t)\Big] - \rho_o q C_{po}\left(\frac{\partial T}{\partial z} - \varphi(z,t) + \frac{gsin(\alpha)}{C_{po}}\right) \tag{10}$$

The term $T_{ext}(z)$ is correlated with the geothermal gradient and L_R is the relaxation-distance parameter that contains the overall heat-transfer coefficient. The parameter $\varphi(z,t)$ considers the Joule-Thomson effect and the kinetic-energy contribution.

Coupling and boundary condition of the wellbore-reservoir system

At the bottom hole, where the wellbore and the reservoir are under the same pressure, temperature, and flow rate, a coupling condition is created between them. At the top of the wellbore, the boundary condition for the flow rate is specified. During the drawdown, the flow rate is set to a constant value q; and during the buildup, it is set to zero, $q = 0$. The reservoir is represented by a Cartesian quadrant, the wellbore is located at a vertex (lower left), in the diagonal opposite to the wellbore (top right, see Fig. 1) the pressure and temperature were set to be constant and no flux conditions for pressure and temperature for the boundary sides.

The initial condition of the wellbore-reservoir system

Before the wellbore top valve is opened, it is assumed the wellbore is filled with oil, so the initial pressure condition is considered to be the hydrostatic gradient. Along the reservoir, the pressure is considered constant (p^0). The wellbore-reservoir system is also assumed to be in local equilibrium with the neighborhood. Therefore, the initial temperature of the reservoir (T^0) is constant, and the wellbore will be the geothermal gradient.

2.2 Inverse Problem

The inverse problem is a well-known issue in the oil and gas industry (Oliver *et al.*, 2008), and this work specifically focuses on history matching. The history matching process aims to estimate parameters that, when inserted into flow simulators, produce responses that fit the observed data. However, due to the high non-linearity of the problem, there may be more than one combination of parameters of interest that result in a similar response to the observed data.

To obtain a range of parameter values as estimations, this work employs ensemble-based methods to solve the history-matching problem. In the literature, various works have addressed history matching problems using genetic algorithms (GA), Ensemble Smoother (ES), Ensemble Smoother with multiple data assimilation (ES-MDA), and other ensemble methods. For instance, Maurya *et al.* (2019) and Xavier *et al.* (2013) employed genetic algorithms for reservoir characterization using different data sources. The ES-MDA method, introduced by Emerick and Reynolds (2013a), has been applied in various works since its development.

Emerick and Reynolds (2013b) compare different ensemble-based methods to evaluate the performance and conclude that ES-MDA provides a better history matching and uncertainty quantification than other ensemble-based methods evaluated. The ES-MDA method is used to estimate and perform the uncertainty analysis of the parameter vector m, which contains reservoir properties. This vector with properties can be generally expressed as:

$$m = [permeabilities,\ porosities,\ dimensions, saturation]^T \tag{11}$$

In order to meet the requirement of ES-MDA, the permeability variable (K) needs to undergo a transformation to the log scale to be expressed in a Gaussian format. Additionally, the variable ϕ represents the homogeneous porosity of the reservoir, as shown in Fig. 1. When the parameter vector (m) is introduced into the flow simulator (g), it generates a response in terms of pressure and temperature (d). The data measured by sensors along the wellbore in the real field is denoted as d_{obs} and represents the data that the history matching process aims to fit. To generate synthetic data that approximates the real data, including measurement noise, Gaussian noise is introduced to the sandface pressure (ϵ_1) and sandface temperature (ϵ_2) data. Therefore, depending on the case, the observed data (d_{obs}) is defined as:

$$d_{obs} = g(m_{true}) + (\epsilon_1 \quad \text{or} \quad \epsilon_2) \tag{12}$$

In the ES-MDA, the observed data (d_{obs}) is perturbed by adding another Gaussian distribution in each assimilation, resulting in d_{uc}. This recurrent procedure, as described by Emerick and Reynolds (2013a) and Emerick and Reynolds (2013b), helps mitigate sampling problems caused by matching outliers that may arise due to perturbations in the observed data (d_{obs}) in nonlinear cases. The equation for d_{uc} is expressed as follows:

$$d_{uc} = d_{obs} + (\alpha_i C_D^{1/2} Z_d)^{1/2}, Z_d = N(0, Id_{N_d}). \tag{13}$$

The variable C_D represents the covariance of the measurement errors matrix. In this work, C_D is considered to be a diagonal matrix. Additionally, α_i represents the inflation coefficient, which satisfies the following equation:

$$\sum_{n=1}^{N_i} \frac{1}{\alpha_i} = 1 \tag{14}$$

The update process of the vector parameters m is defined as follows, where the superscripts a represent the present ensemble and p represent the prior ensemble. The subscript j denotes the ensemble counter, ranging from 1 to N_e individuals.

$$m_j^a = m_j^p + [C_{MD}(C_{DD} + \alpha_i C_D)^{-1}](d_{uc} - d_j^p) \tag{15}$$

The matrices C_{MD} and C_{DD} are defined as follows, representing the cross-covariance between the parameters and the simulated data, and the auto-covariance matrix of the simulated data, respectively:

$$C_{MD} = \frac{1}{N_e - 1} \sum_{j=1}^{N_e} (m_j^f - \overline{m}^f)(d_j^f - \overline{d}^f)^T \tag{16}$$

$$C_{DD} = \frac{1}{N_e - 1} \sum_{j=1}^{N_e} (d_j^f - \overline{d}^f)(d_j^f - \overline{d}^f)^T \tag{17}$$

In both equations, N_e represents the ensemble size, and the overline marker indicates the mean of the variable.

Numerical Formulation

The Equation 3 to Equation 10 are discretized using the implicit Crank-Nicolson method to approximate time derivatives and second-order finite difference to approximate spatial derivatives. A hyperbolic function was used to refine the reservoir mesh near the well and a uniform distribution is used in the well domain. The step time follows a Sigmoid function that increases smoothly from 10^{-6}s to 60s.

Results

3. Synthetic Data - Direct Problem

After performing mesh tests and validating the model with results from a non-isotherm radial simulator and with analytical pressure results, several simulations were performed with varying porosity, permeability, and position where the permeability changes. Below we present some configurations that will be used together with the inverse problem methodology. All simulations were performed during the flux period (48 hours), with a constant flow rate of $800m^3/day$. In this work, three reservoir configurations will be presented: a homogeneous reservoir, a reservoir with two different permeabilities, and another containing a region with high permeability. The last two configuration are shown in Figure 2. The permeabilities of the reservoir are set as follow, Case 1 represents a Homogeneous reservoir with $K_1 = K_2 = K_3 = 100mD$, Case 2 with $K_1 = 100mD$, and $K_3 = K_2 = 1000mD$ where $x1 = 9.00$ m, and the last Case 3 with

Figure 2: Different analyzed Cartesian reservoir configurations. Case 2 (left) includes two different permeability regions delimited by x_1. Case 3 (right) consists of three permeability regions delimited by positions x_1 and x_2.

Table 1: Reservoir properties, constants, and wellbore properties used in the analyzed cases

Property	**Units**	**Value**	Property	**Units**	**Value**
L	m	$2,500.0$	r_w	m	0.156
ϕ	fraction	0.12	r_{co}	m	0.12224
c_r	cm^2/kgf	3.0e-5	r_{ci}	m	0.10839
s_w	fraction	0.15	r_{to}	m	0.06985
g_t	K/m	0.03	r_{ti}	m	0.05931
$c_p r$	$J/m^3/K$	2.347e+6	λ_{cem}	$J/m/h/K$	6.833e+3
λ_r	J/m/K	1.396e+4	λ_{wall}	$J/m/h/K$	1.617e+5
λ_e	J/m/K	1.396e+4	$\lambda_{wall-cem}$	$J/m/h/K$	9.995e+3
α_e	m^2/h	5.894e-3	λ_{an}	$J/m/h/K$	5.833e+2
λ_t	$J/m/h/K$	1.238e+4	Skin factor	-	0
ϕ_t^*	$K/(Kgf/cm^2)$	1.874e-3	θ	$degree$	90^0
α_t	m^2/h	5.342e-3	-	-	-

Table 2: Fluid properties of oil and water used in the analyzed cases

Property	**Units**	**Oil**	**Water**
B	$m^3/stdm^3$	1.4	1.0
c	cm^2/kgf	1.10e-4	3.96e-5
μ	cP	0.9	1.0
λ	$J/m//h/K$	5.833e+2	2.229e+3
ρ	Kg/m^3	770.0	998.2
β	K^{-1}	1.11e-3	5.27e-4
c_p	$J/Kg/K$	2252.9	4209.35
ε_{JT}	$K/Kgf/cm^2$	-3.374e-2	-1.921e-2
φ	$K/(Kgf/cm^2)$	2.279e-2	4.132e-3

$K_1 = K_3 = 100mD$, $K_2 = 1000mD$. Here $x1 = 9$m and $x2 = 65$ m. Table 1 exhibit the reservoir and wellbore parameter's inputs. While Tab. 2 details the properties of the fluids.

Figure 3 and Figure 4 shows a diagnostic plot (Bourdet derivative) for all cases. Numerical prediction related to pressure data is shown in Figure (3) and as expected, the homogeneous reservoir achieve a characteristic response, i.e. a single plateau (in Blue). Prediction from second case delivers two plateaus suggesting two different region from a lower to high permeability (in red). The third case, the pressure derivative start from the initial same plateau level and then start to decrease suggesting a region of high permeability and then before to achieve the second plateau it start to increase toward to initial plateau. From this last case, the diagnostic plot suggest three different region.

On the other hand, temperature data in a diagnostic plot shows a single plateau for all cases, suggesting that the signal temperature has achieve only the region close to the well. Two days of oil production is not enough to cover the transition

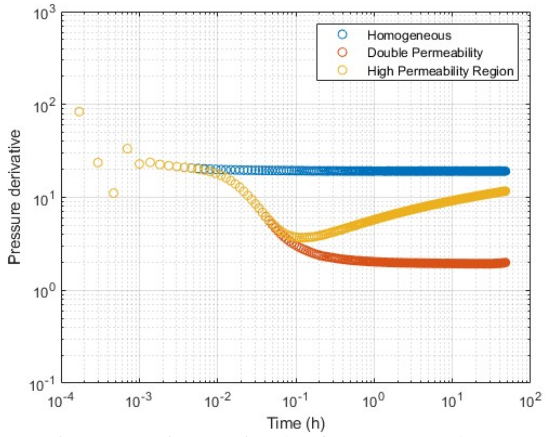

Figure 3: Diagnostic plot for pressure data.

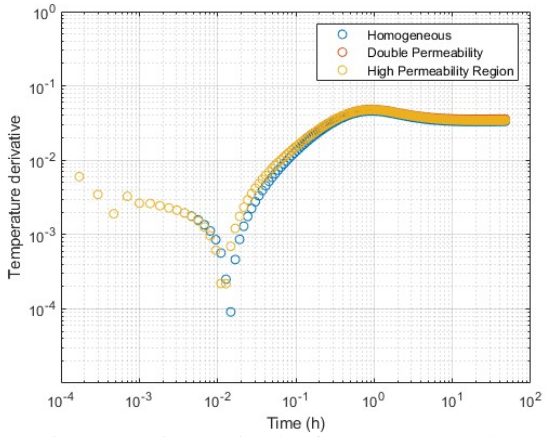

Figure 4: Diagnostic plot for temperature data.

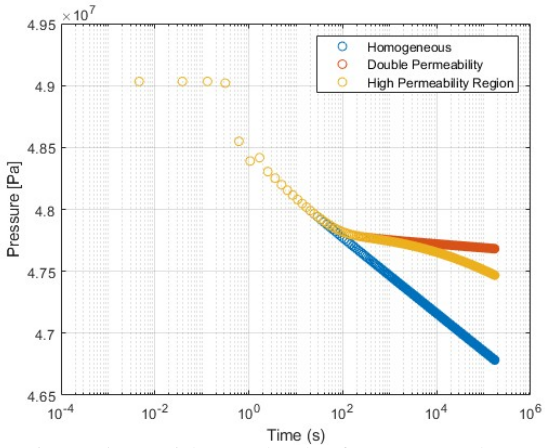

Figure 5: Semi-log scale plot for pressure data.

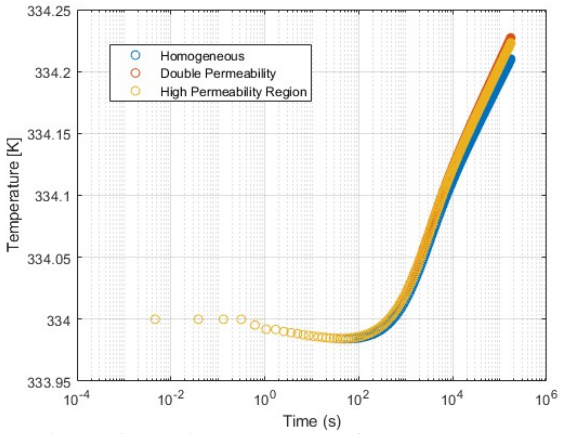

Figure 6: Semi-log scale plot for temperature data

zone located at $x1 = 9$m. The main limitation of temperature analysis is the length of test duration that directly impacts the investigation radius. Temperature data help in the characterization of the reservoir for regions close to the wellbore, since the thermal effects are confined in this area. Temperature data is also important to help in determining the porosity since changes in this property are more sensitive in temperature derivative graphs.

A similar conclusion can be obtained by analyzing the semi-log scale graph, as shown in Figures 5 and 6. Analyzing the semi-log plot for pressure data, Case 2 in Figure 5 shows a change in the slope along the time (in red) in reference of the homogeneous case (in blue), suggesting a region with different permeability, in case 3 there is a same change in the slope, but again there is an attempt to return to the original slope. For temperature data in a semi-log scale graph, all those three cases follow the same trend. This behavior is expected because the temperature signal is associated to the same region close to the well, for all cases.

4. INVERSE PROBLEM

The ES-MDA method uses pressure and temperature data obtained from the Cartesian simulator to best fit an observed data (d_{obs}). The observed data is a synthetic data previously obtained considering a Gaussian noise. Table 3 shows the parameters to be estimated such as the permeability of those three region in natural logarithm scale, and porosity. Because we are dealing with a stochastic method, we present the mean and standard deviation from the initial state to the final state which the process is converged, as shown on the right of the Table 3.

Figures 7 and 8 show the evolution of pressure and temperature convergence for each step of the ES-MDA's method process. It is important to notice that the solution is not unique, different reservoir configurations can lead to identical pressure and temperature responses.

Figures 9a and 10a show the final distribution of each permeability and porosity after three steps of the ES-MDA method. A good parameter prediction was achieved for the case 3 by using this method.

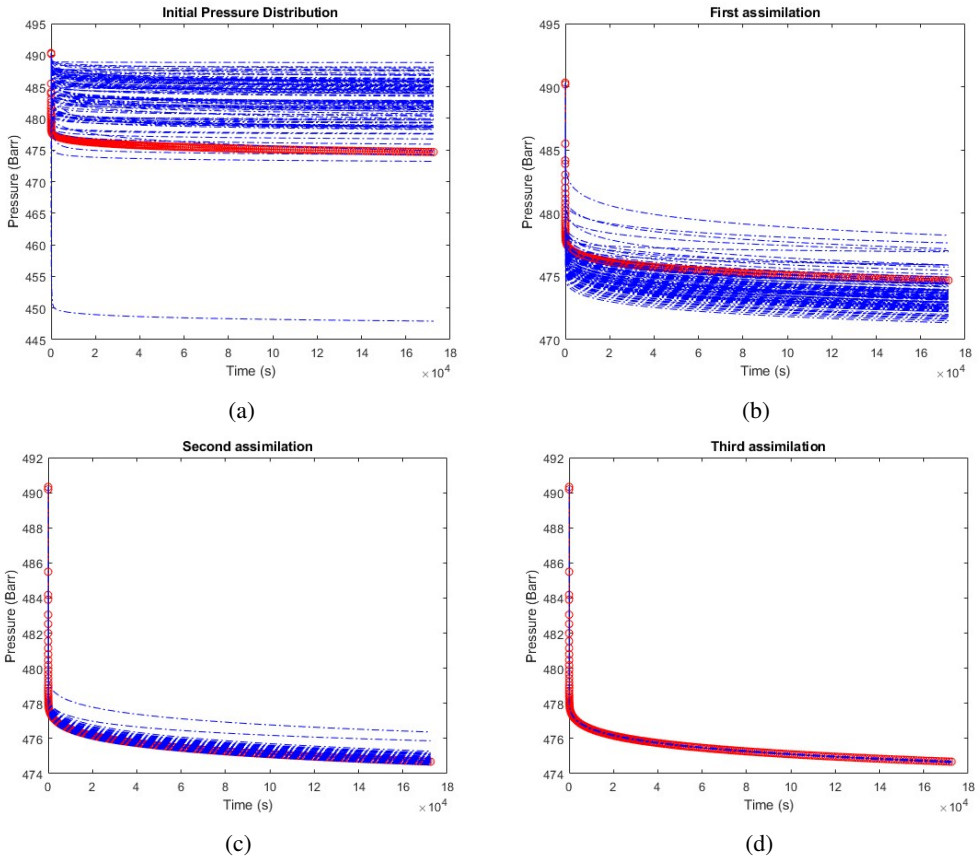

Figure 7: Convergence process of pressure through ES-MDA method. The red line is the target pressure, while the blue one is the pressure estimated for each step.

Table 3: Summary of the initial distribution parameters used in the ES-MDA, target values, and estimated mean values.

Parameter	**initial mean**	**initial STD**	**Target**	**obtained mean**
Log (K1)	6 (403 mD)	0.8	4.605 (100 mD)	4.603 (99.81 mD)
Log (K2)	6 (403 mD)	0.8	6.908 (1000 mD)	6.878 (970.36 mD)
Log (K3)	6 (403 mD)	0.8	4.605 (100 mD)	4.551 (94.74 mD)
ϕ	0.2	0.04	0.12	0.138

5. CONCLUSIONS

In this work was developed a simulator based on a Cartesian-reservoir considering Joule- Thompson heating/cooling, adiabatic fluid expansion/compression, conduction, and convection effects for both wellbore and reservoir for a single-phase fluid flow. The use of a Cartesian system to describe the reservoir allows the study of new configurations extending the radial analysis. Different permeability configurations were tested in order to analyze the pressure and temperature data using a semi-log and derivative plots.

The inverse problem of a formation test to estimate parameters of the reservoir was solved by using ES-MDA method. Results show that the ES-MDA method applied with the coupled pressure and temperature transient data provides good reservoir characterization and uncertainty quantification.

6. REFERENCES

Emerick, A.A. and Reynolds, A.C., 2013a. "Ensemble smoother with multiple data assimilation". *Computers & Geosciences*, Vol. 55, pp. 3–15. ISSN 0098-3004. doi:https://doi.org/10.1016/j.cageo.2012.03.011. Ensemble Kalman filter for data assimilation.

Emerick, A.A. and Reynolds, A.C., 2013b. "Investigation of the sampling performance of ensemble-based methods with a simple reservoir model". *Computational Geosciences*, Vol. 17, No. 2, pp. 325–350.

Galvao, M.S., Carvalho, M.S. and Barreto Jr, A.B., 2020. "Thermal impacts on pressure transient tests using a coupled

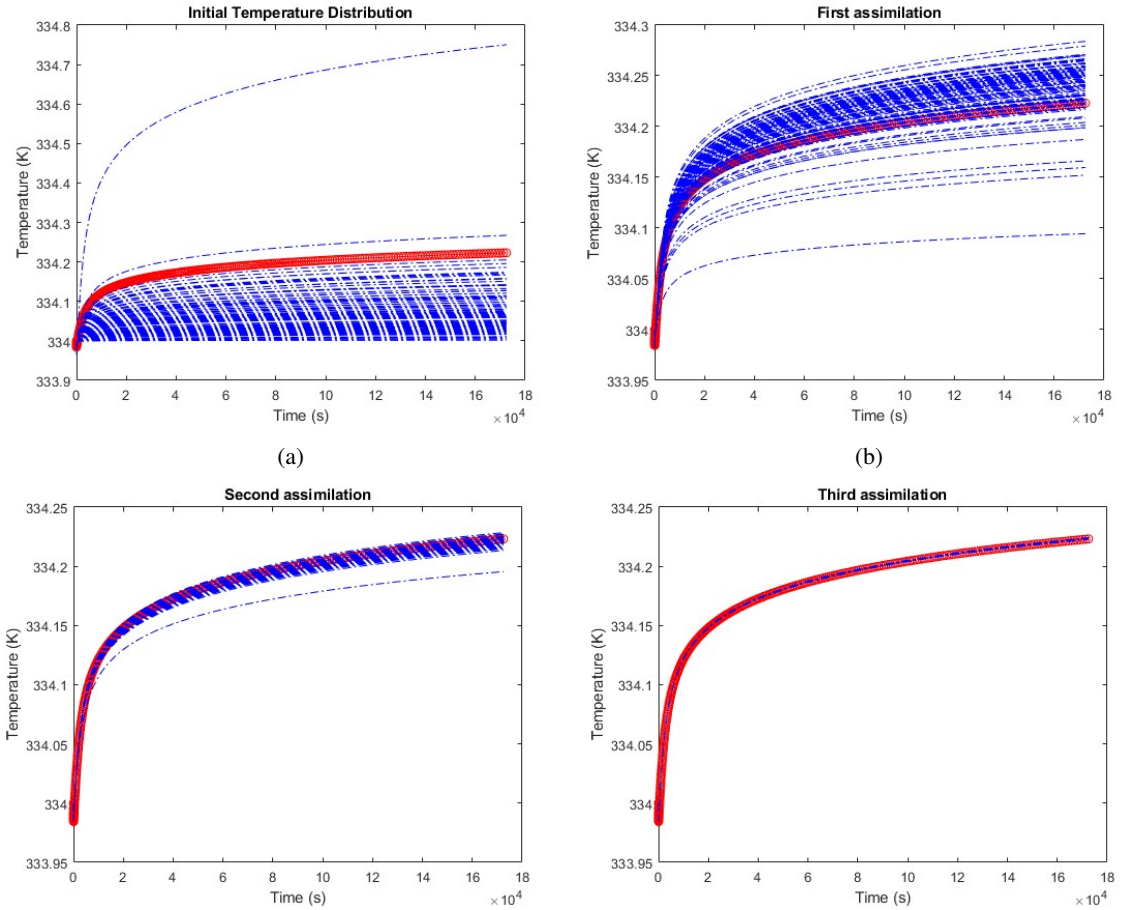

Figure 8: Convergence process of temperature through ES-MDA method. The red line is the target temperature, while the blue ones are the temperature estimated for each step.

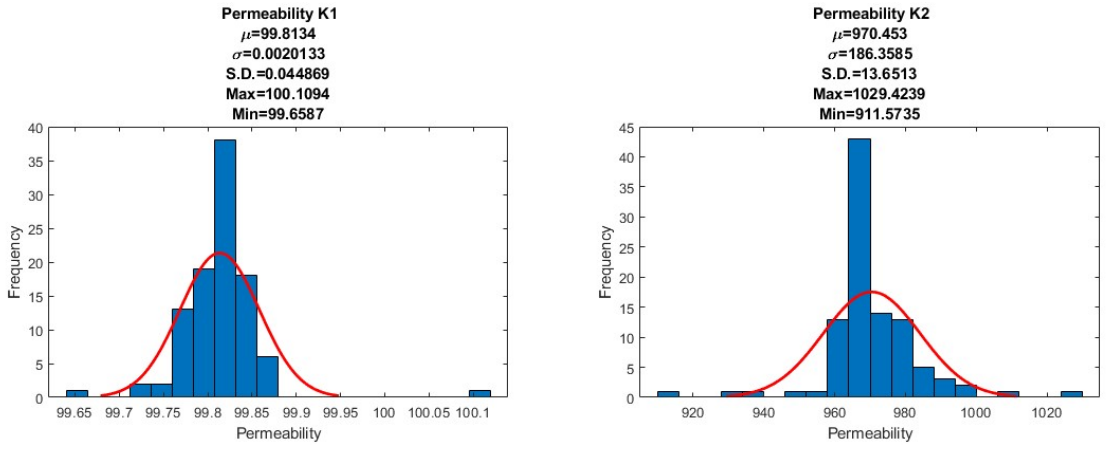

Figure 9: Histogram with the permeability distribution estimated in Case 3. (A) is the first permeability region (K_1), and (B) is the second permeability region (K_2).

wellbore/reservoir analytical model". *Journal of Petroleum Science and Engineering*, Vol. 191, p. 106992.

Hasan, A.R. and Kabir, C.S., 2005. "A simple model for annular two-phase flow in wellbores". In *SPE Annual Technical Conference and Exhibition*. Society of Petroleum Engineers.

Mattoso R. da Silva, V., 2022. *Reservoir characterization based on pressure and temperature transient data, using an ensemble-based method*. Ph.D. thesis, PUC-Rio.

Maurya, S.P., Singh, N.P. and Singh, K.H., 2019. "Use of genetic algorithm in reservoir characterisation from seismic

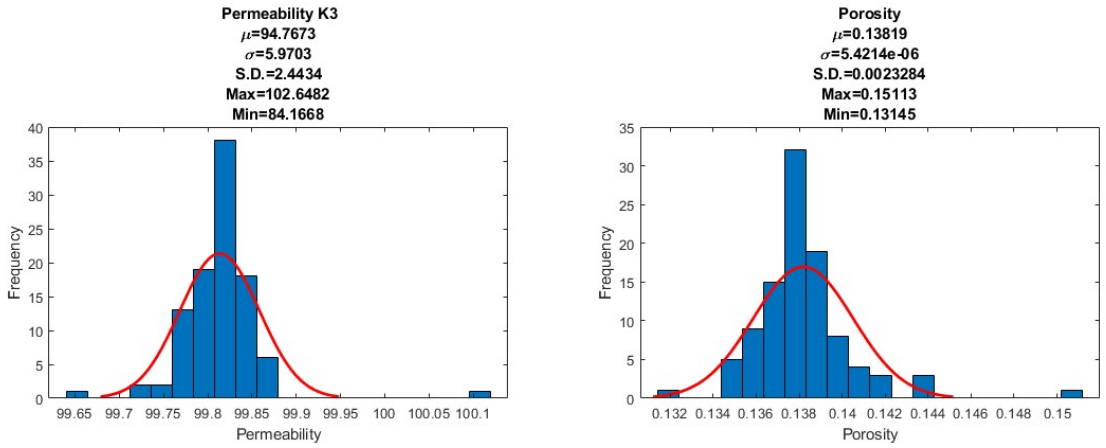

(a) (b)

Figure 10: Histogram with the permeability and porosity distribution estimated in Case 3. (A) is the third permeability region (K_3), while (B) is the porosity (ϕ).

data: A case study". *Journal of Earth System Science*, Vol. 128, pp. 1–15.

Oliver, D.S., Reynolds, A.C. and Liu, N., 2008. *Inverse theory for petroleum reservoir characterization and history matching*.

Onur, M. and Cinar, M., 2017. "Analysis of sandface-temperature-transient data for slightly compressible, single-phase reservoirs". *Spe Journal*, Vol. 22, No. 04, pp. 1134–1155.

Onur, M., Ulker, G., Kocak, S. and Gok, I.M., 2017. "Interpretation and analysis of transient-sandface-and wellbore-temperature data". *SPE Journal*, Vol. 22, No. 04, pp. 1–156.

Park, H. and Horne, R., 1989. "Well test analysis of a multilayered reservoir with formation crossflow". In *SPE Annual Technical Conference and Exhibition*. OnePetro.

Sui, W., Zhu, D., Hill, A.D. and Ehlig-Economides, C.A., 2008. "Determining multilayer formation properties from transient temperature and pressure measurements". In *SPE Annual Technical Conference and Exhibition*. OnePetro.

Xavier, C.R., dos Santos, E.P., da Fonseca Vieira, V. and dos Santos, R.W., 2013. "Genetic algorithm for the history matching problem". *Procedia Computer Science*, Vol. 18, pp. 946–955.

7. RESPONSIBILITY NOTICE

The author(s) is (are) solely responsible for the printed material included in this paper.